Drying Technology: An International Journal
Publication details, including instructions for authors and subscription information:
http://www.tandfonline.com/loi/ldrt20

A Funtadamental Study on Particle Transport Through Rotary Dryers for Flight Design and System Optimisation

F.Y. Wang [a], I.T. Cameron [a], J.D. Litster [a] & V. Rudolph [a]
[a] Department of Chemical EnnineeringThe University of Queensland, Queensland, 4072, Australia
Published online: 19 Oct 2007.

To cite this article: F.Y. Wang, I.T. Cameron, J.D. Litster & V. Rudolph (1995) A Funtadamental Study on Particle Transport Through Rotary Dryers for Flight Design and System Optimisation, Drying Technology: An International Journal, 13:5-7, 1261-1278, DOI: 10.1080/07373939508917021

To link to this article: http://dx.doi.org/10.1080/07373939508917021

DRYING TECHNOLOGY, 13(5-7), 1261-1278 (1995)

A FUNDAMENTAL STUDY ON PARTICLE TRANSPORT THROUGH ROTARY DRYERS FOR FLIGHT DESIGN AND SYSTEM OPTIMISATION

F.Y. Wang, I.T. Cameron, J.D. Litster and V. Rudolph
Department of Chemical Engineering
The University of Queensland
Queensland, 4072 Australia

Key Words: differential calculus, flight geometry, rotary dryer, solid transport, optimisation

ABSTRACT

A model for particle transport in a flighted horizontal rotary dryer is developed in this paper. Mathematical principles applied to the current study are in the areas of differential calculus and analytical geometry. In contrast to the conventional approaches which are either based on empirical/semi-empirical correlations or obtained from the investigation of single particle trajectories, this paper develops rigorous mathematical analysis of the transport of bulk solids. A variety of important issues in rotary drying, such as axial flowrate of solids, retention time distribution and solid holdup are addressed and treated by using non-traditional methods. Since the model takes dimension, number and geometry of flights into account, it possesses the following two characteristics : (1) it is not only useful in the study of rotary drying dynamics, but also applicable to other processes employing flighted rotating cylinders (such as granulation drums and crushers); and (2) based on the model, an optimal drum configuration can be designed by using optimisation techniques. The model can be incorporated within a distributed parameter dryer model developed previously to form a more rigorous integrated dynamic model. A theoretical foundation for optimal flight design by using the current model is explained.

A pilot scale perspex rotary dryer equipped with a video camera has been constructed and used for model validation. Raw sugar was handled in the experiments. Particle transport was observed and measured by using a flow visualisation technique supplemented with traditional sampling methods. A significant model quality improvement has been observed through a comparative study between the newly developed model and conventional ones.

Flighted rotary drums are very widely used in the drying industry, amongst others. A cross sectional view of a typical flighted rotary dryer is schematically shown in Figure 1. A distributed parameter dryer model described by a set of partial differential equations has been developed recently by the authors (1 and 2). A key aspect in understanding the rotary dryer operation, is a knowledge of the solid transport behaviour, including retention time distribution, discharge rates from flights, axial solid flowrate, geometry and voidage of airborne curtains, and particle holdup. Consequently, a number of investigators such as Kelly et al. (3), Glikin (4), Kamke et al. (5), Matchett et al. (6), Gupta et al. (7) and Sherritt et al. (8) have been attracted by these topics. Notable developments have been reported in recent years but gaps in knowledge remain. These include:

(1) Rigorous mathematical derivations were not emphasised in many papers. For example, the following three defects can be detected in recent publications:

(a) The infinitesimal representation of discharge volume from a flight given by

$$dV = \ell^2 \, d\theta/2 \qquad (1)$$

developed by Sherritt (8) will lead to considerable errors because of the geometry simplification. The Sherritt equation is correct for the auxiliary circle centred at the point C in Figure 2 rather than for the circle representing the drum wall.

(b) The average value approach (average falling angle and height) given by

$$\bar{\theta} = \frac{\int_0^{V_0} \theta \, dV}{V_0} \; ; \; \bar{h} = R_{eff}(1+\sin \bar{\theta}) \qquad (2)$$

is extensively used in particle transport simulations, but this is obviously inadequate where there are high dispersions about the average.

(c) Significant computational errors may occur by discretizing volume V in commonly used numerical schemes for the evaluation of integral equations (such as average angle representation in Equation (2)). This is because the variation of volume V may become a higher order infinitesimal than variation of angle θ in some regions.

(2) A generalised approach handling flights with arbitrary geometry has not been developed.

(3) Particle transport and dryer dynamics were studied separately. A unified theory and algorithm to integrate these two stages has yet to be developed.

A generalised model for particle transport in flighted rotary dryers aimed at partly filling the identified gaps is developed in this work, by employing a rigorous mathematical analysis in areas of differential calculus and analytical geometry. This particle transport model is a constituent of the overall dynamic model described by partial differential equations.

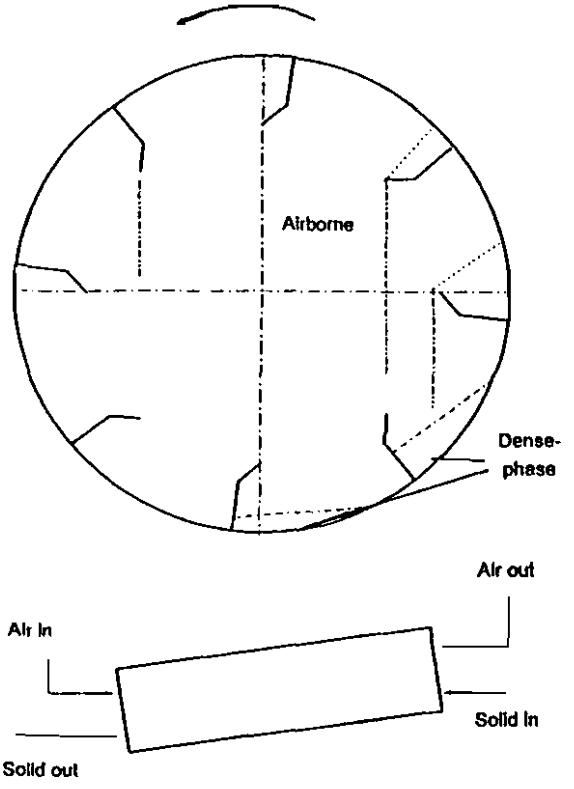

Figure 1: A Flighted Rotary Dryer

SOLID FLOWRATE AND RETENTION TIME

A simplified cross sectional view of a rotary dryer is shown in Figure 3 in which ϕ is denoted as the kinetic angle of repose and the angle θ determines the position of a flight. If both ϕ and θ are specified, the cross sectional area filled with particles in the flight is computable by using analytical geometry for irregularly shaped flights or plane geometry for regularly shaped ones. Consequently, the solid holdup in the flight is uniquely *determined in terms of the flight geometry, position and kinetic angle of repose. Normally* at least three parameters are required to described a flight with simple geometry: two side lengths h and d, and angle α formed by these two sides (Figure 3). The kinetic angle of repose ϕ is a function of the static friction coefficient μ, position θ and angular velocity ω.

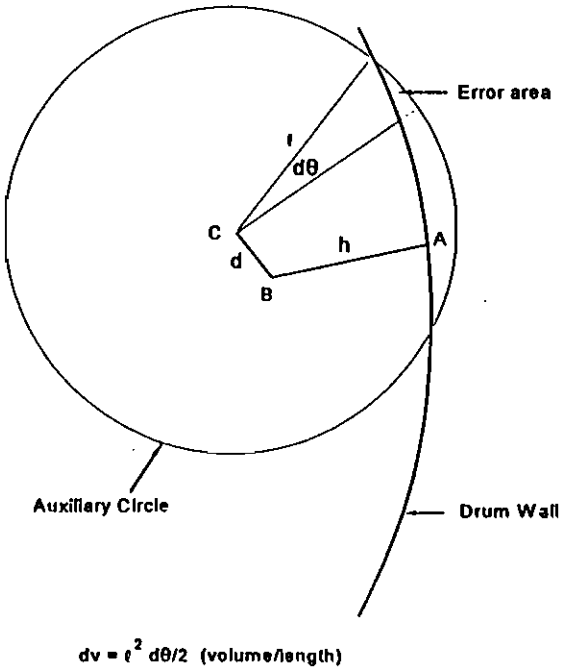

Figure 2: Error Detection for Simplified Method

The following correlation is well regarded and widely accepted (4 and 10):

$$\tan \phi = \frac{\mu - \mu(\omega^2 R/g)\sin\theta + (\omega^2 R/g)\cos\theta}{1 - \mu(\omega^2 R/g)\cos\theta - (\omega^2 R/g)\sin\theta} \qquad (3)$$

That is, if the flight geometry is specified, the cross sectional area of a flight filled with solids is a composite function of θ ($S = S(\theta,\phi(\theta))$). The correlation given by Equation (3) has been validated for sugar particles (10) which will be used in an application example reported in this work. In optimisation studies, the number, dimensions and geometry of flights are treated as parameters to be determined by using mathematical programming. In this case, the cross section area S should be represented as $S = S(\theta,\phi(\theta); h,d,\alpha)$.

When the drum is rotating, the infinitesimal angle and time are related by:

$$d\theta = \omega dt \qquad (4)$$

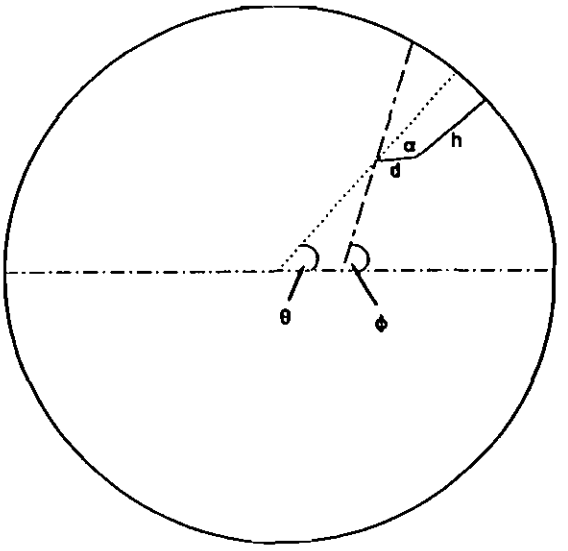

Figure 3: View of A Simplified Rotary Drum

The particle discharge rate from the ith flight is then given by:

$$R_{Di} = -\rho_b \omega \frac{dS_i}{d\theta_i} = -\rho_b \omega \left(\frac{\partial S_i}{\partial \theta_i} + \frac{\partial S_i}{\partial \phi_i} \frac{\partial \phi_i}{\partial \theta_i} \right) \quad (5)$$

The axial solid flowrate can be obtained by using the discharge rate in the vertical direction given by Equation (5). Figure 4 shows the side view of a dryer. The particle transport is illustrated by two disks (Disks 1 and 2) displayed in the figure, with one (Disk 1) perpendicular to the drum axis and the other vertical (Disk 2). The infinitesimal slices used in the development of heat and mass transfer equations (1 and 2) are perpendicular to the drum axis. It is easy to see from Figure 4 that the far extreme points in flights delivering particles to the next slice bounded by Disk 1 are on Disk 2. That is, the mass passing through Disk 1 is determined by the amount of particles discharged from the segments of flights between Disks 1 and 2 with the lengths L_i, $i = 1, 2, \ldots, n$. In the example shown in Figure 4, since there are four active flights, the lengths L_1, L_2, L_3 and L_4 should be determined. The axial solid flowrate consists of both the airborne particle delivery (particles penetrating the inclined Disk 1) and the dense phase kilning. If the axial drag force is negligible, the solid flowrate is given by:

$$V_s = \Gamma \sum_i (R_{Di} L_i) = \Gamma \omega \rho_b \sum_i \left(\frac{dS_i}{d\theta_i} L_i \right) \quad (6)$$

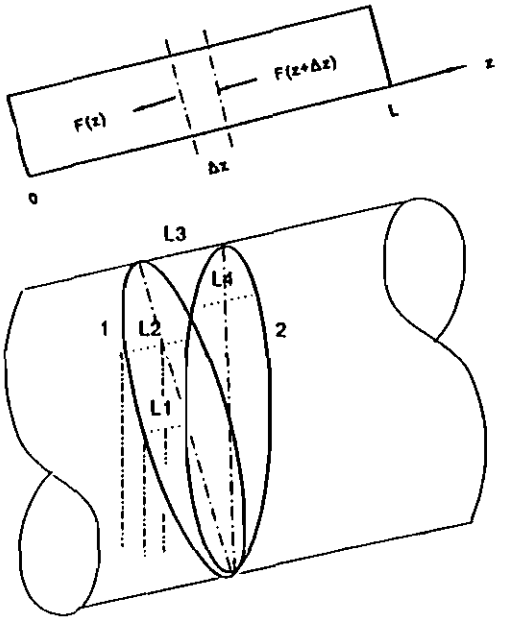

Figure 4: Side View of Rotary Dryer

where $\Gamma \geq 1$ is a correction factor taking the kilning effect into account, and the length L_i in the ith flight delivering particles to the next infinitesimal slice can be computed as follows:

$$L_i = h_i \tan \gamma \tag{7}$$

A more rigorous mathematical treatment on the kilning effect is continuing which will be reported in our subsequent papers. It should be pointed out that the height h_i, defined as the distance between the discharging point from the ith flight and the bottom dense phase, must also be computed dynamically. A commonly used simple equation given by $h_i = R_{eff}(1+\sin \theta_i)$ is a poor approximation in which the shape complexity of the dense phase is not taken into account. When axial drag force is not negligible, the following equations can be used to correct the length L_i:

$$\begin{aligned} \bar{L}_i &= L_i - \frac{1}{2} a t_i^2 \\ t_i &= \sqrt{\frac{2h_i}{g}} \\ a &= C_D \frac{\pi \rho_a V_P^2 D_P^2}{8 m_P} \end{aligned} \tag{8}$$

where the drag coefficient can be determined by using correlations explained in Denn (11).

The solid transport model developed this way is incorporated with the heat and mass transfer models developed earlier by the authors (1 and 2). This forms a combined distributed parameter model. All the distributed variables can be computed more accurately by using the combined model than previously done. For example, the solid phase mass balance given by:

$$\frac{\partial M_s}{\partial t} = \frac{\partial V_s}{\partial z} \tag{9}$$

can be used to compute the solid holdup in combination with the axial solid flowrate as explained above. From Equation (9), a mathematical representation of the retention time is derived as:

$$t_r(t) = \int_0^L \frac{\partial M_s}{\partial V_s}\, dz \tag{10}$$

Since the axial solid flowrate can be computed rigorously, the retention time described by Equation (10) is not explicitly used in dynamic simulations. It is useful in the estimation of operational conditions by practitioners and in the equipment design.

In this section, most of the derivations are done using differential calculus. Symbolic mathematics software, such as MAPLE, MATHEMATICA, MATLAB with Symbolic Math Toolbox, and Calculus Calculator (CC4) is needed for the calculations, in particular for solving Equation (5).

AIRBORNE HOLDUP

In our previous work, the airborne holdup was determined by using the Hironsue's correlation (9) which was originally developed for some special cases. More recently, Sherritt (8) proposed a computational method in which the total airborne holdup was computed as the product of the average airborne holdup for one flight and the total number of flights. As pointed out previously, considerable errors can be incurred by using an average value approach. A method for accurate computation of airborne holdup should be developed.

Since the particle discharge rate from a flight at any position is computable by using the techniques developed in the previous section, the instantaneous total airborne holdup can be obtained as follows:

$$G_a = \sum_i R_{Di}\, t_i \tag{11}$$

where the particle falling time, t_i from the ith flight is given in Equation (8). This assumes

that (a) the initial vertical velocity is zero; (b) the vertical drag force is negligible; and (c) there is no hindrance from other particles. If Assumptions (a) and (b) are not valid, the following equation should be used:

$$h_i = v_0 t_i + \frac{1}{2}(g - a_v) t_i^2 \tag{12}$$

where a_v is computed in a similar way as the last equation in Equation (8) and the extreme values of the initial vertical velocity v_0 will be determined in the next section.

CURTAIN GEOMETRY AND VOIDAGE

The size and shape of curtains formed by discharged particles from flights are determined by using the extreme value theory based on an analysis of single particles in extreme conditions. The extreme single particle motions are shown schematically in Figure 5. The maximum initial velocity of a single particle from a flight is the result of the angular velocity and a sliding/rolling velocity along the solid surface in the flight. This resultant velocity can be further decomposed into horizontal and vertical velocities, v_h and v_v, described by the following equation:

$$\begin{aligned} v_h &= \omega R_t \sin\theta + \sqrt{2gl(\sin\phi - \zeta\mu\cos\phi)}\cos\phi \\ v_v &= -\omega R_t \cos\theta + \sqrt{2gl(\sin\phi - \zeta\mu\cos\phi)}\sin\phi \end{aligned} \tag{13}$$

where R_t is the distance from the centre of the drum to the tip of a flight and the parameter $\zeta \leq 1$ is determined based on the relative importance between sliding and rolling motions. The width of the curtain at any specified vertical distance h_t from the flight lip is given by:

$$\begin{aligned} W_c &= v_h t_v \\ v_v t_v + \frac{1}{2} g t_v^2 &= h_t \end{aligned} \tag{14}$$

The average voidage of the ith curtain, ϵ_i, is described as:

$$\varepsilon_i = \frac{A - \frac{R_{mi} t_i}{\rho_s}}{A} = 1 - \frac{R_{mi} t_i}{\rho_s A} \tag{15}$$

where ρ_s is the actual solid density, t_i is the particle falling time from the ith flight and A is the cross section area of the ith curtain. The equations formulated in this section will be validated against the experimental data.

OUTLINE OF A POSSIBLE OPTIMISATION STRATEGY

Since the number and geometry of flights are considered in the development of the mathematical models for particle transport in rotary dryers, the models can be used in the design of optimal dryer configurations. A detailed description of system optimisation by

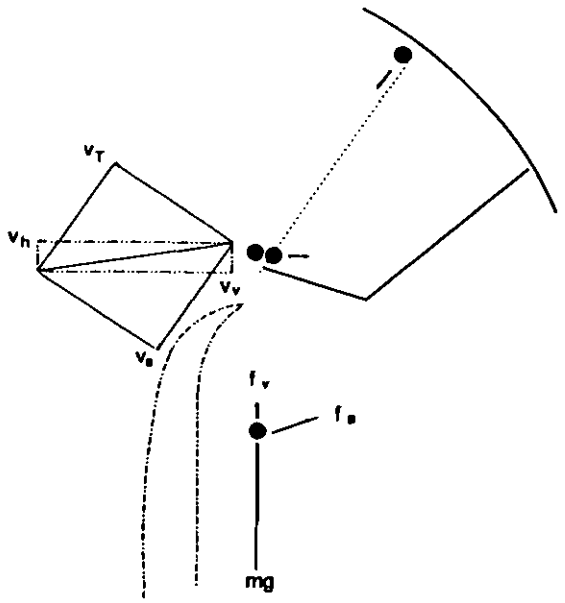

Figure 5: Curtain Geometry Analysis—
Extreme Value Theory

using the current models exceeds the scope of this paper. Only the principles used in the system optimisation are outlined. As pointed out previously, the discharge rate R_{Di} from the ith flight is not only a function of position θ_i, but also a function of the flight configuration in terms of h, d and α. Consequently, the width of the ith curtain, W_{ci}, given by Equation (14) is also a function of h, d and α. In practice, the active heat and mass transfer volume in the dryer should be as large as possible to achieve maximum drying efficiency. The constrained optimisation problem can be formulated as follows:

$$\underset{h,d,\alpha}{\text{Maximize}} \left\{ \sum_{i=1}^{n} \left(W_{ci}(\theta_i;\ h,d,\alpha) + w_i\, R_{Di}(\theta_i;\ h,d,\alpha) \right) \right\} \qquad (16)$$

subject to the constraints given by Equations (5) and (14). The active flight number n in Equation (16) depends on the total flight number N. The optimisation problem can be solved by employing a mathematical programming approach with four decision variables: h, d, α and N.

PILOT PLANT CONFIGURATION

A pilot scale flighted rotary dryer equipped with a video camera, video recording system and television has been built to validate the model. An air chamber and a fan are also

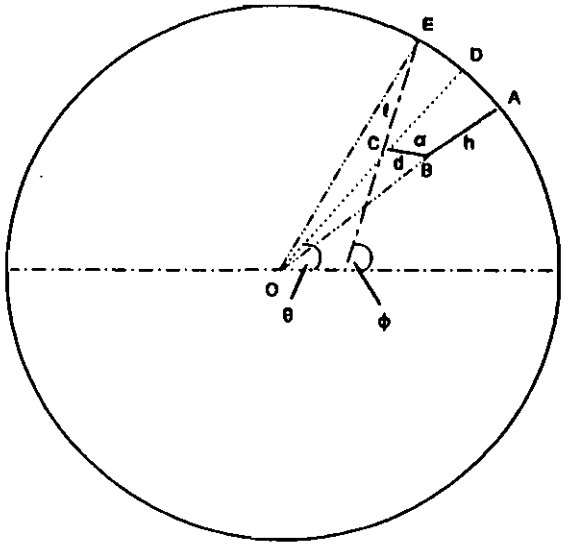

Figure 6(a): Cross Section Area at Stage 1

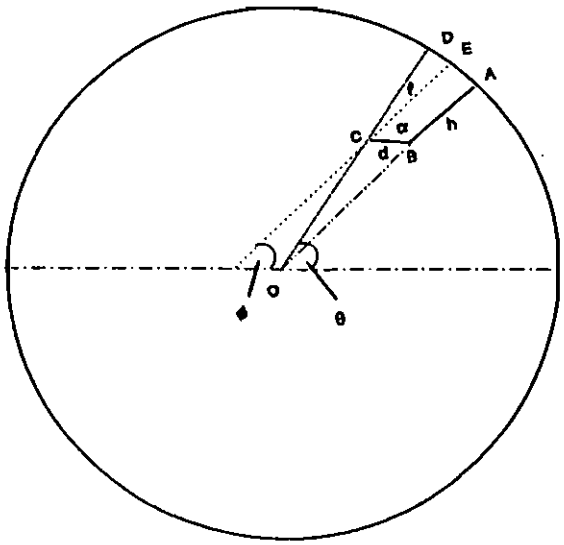

Figure 6(b): Cross Section Area at Stage 2

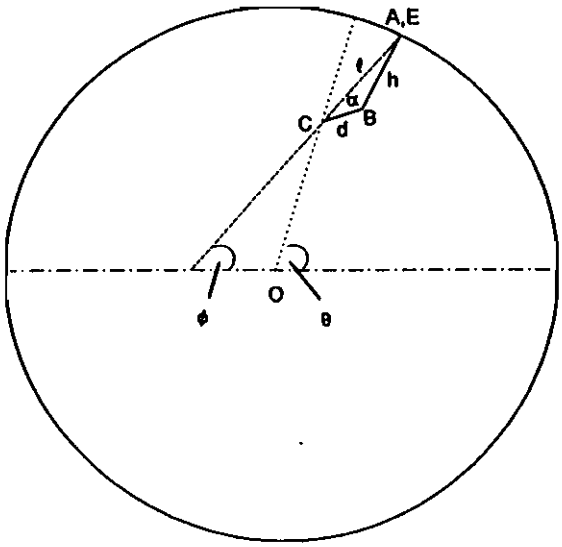

Figure 6(c): Bounding Point

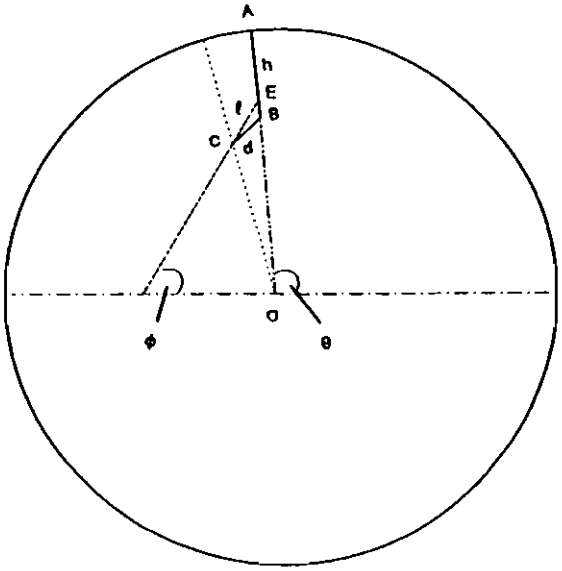

Figure 6(d): Cross Section Area at Stage 3

connected to the dryer to introduce air flow through the drum. Raw sugar is used as the testing material. The pilot dryer parameters are as follows (refer to Figure 3):

D = 0.3m, L = 1.75m, h = 0.03m, d = 0.02m, α = 105°, Number of Flights = 10
Rotation Rate = 0 to 16 rpm, Inclination Angle (γ) = 0° to 8°
Friction Coefficient of Sugar = tan 40° to tan 60° (from (10))
Air velocity = 0 to 1.5 m/s

A more detailed description on the pilot plant design and experimental procedures is available elsewhere (12 and 13).

A time consuming step in the application of techniques developed in this paper is to formulate representations of cross section areas filled with particles in order to use Equation (5). The flight design shown in Figure 6 is used to demonstrate the computational procedures. The following three cases may be distinguished in computations: $0 \le \theta \le \phi$; $\phi \le \theta \le \theta_s$; and $\theta_s \le \theta \le \theta_f$, where θ_s represents the bounding angle at which the shape of cross section filled with solids, changes from a quadrilateral to a triangle (Figure 6(c)), and θ_f is the final angle at which the particles are completely discharged. The most important parameter to be determined is the side length ℓ (CE in Figure 6). In Stage 1 (Figure 6(a)), ℓ = CE is computed by using:

$$\overline{CE}^2 + 2\,\overline{CO}\,\overline{CE}\cos(\phi-\theta) + (\overline{CO}^2 - R^2) = 0 \qquad (17)$$

where

$$\overline{CO}^2 = \overline{BC}^2 + (R-\overline{AB})^2 + 2\overline{BC}(R-\overline{AB})\cos\alpha \qquad (18)$$

The cross section area filled by particles in Stage 1 is given by:

$$S = \frac{1}{2}R^2\angle AOE - \text{area}(\triangle COB + \triangle COE) \qquad (19)$$

where

$$\text{area}(\triangle COB) = \frac{1}{2}\,\overline{CE}\,\overline{CO}\sin(\angle OCE)$$
$$\text{area}(\triangle COE) = \frac{1}{2}\,\overline{BC}\,\overline{CO}\sin(\angle OCB) \qquad (20)$$

In Stage 2 (Figure 6(b)), ℓ = CE is determined as:

$$\overline{CE}^2 + 2\,\overline{CO}\,\overline{CE}\cos(\phi-\theta) + (\overline{CO}^2 - R^2) = 0 \qquad (21)$$

The shifting angle θ_s (Figure 6(c), E coincides with A) is computable by using the following equation:

$$\overline{AB}^2+\overline{BC}^2-2\ \overline{AB}\ \overline{BC}\cos\alpha = -[2\ \overline{AC}\ \overline{CO}\cos(\theta_4-\phi)+(\overline{CO}^2-R^2)] \quad (22)$$

The area filled with particles in Stage 2 is represented by:

$$S = \left[r\ (r-\overline{CE})\ (r-\overline{CO})\ (r-R)\right]^{1/2} + \frac{1}{2} R^2\ \triangle AOE - \text{area}(\triangle BOC) \quad (23)$$

where

$$r = \frac{1}{2}\ (\overline{CE}+\overline{CO}+R) \quad (24)$$

$$\triangle AOE = \triangle AOD - \arcsin\ (\overline{CE}\sin(\theta-\phi)/R)$$

Stage 3 is shown in Figure 6(d) with side length $\ell = CE$ described by:

$$\ell = \overline{CE} = \frac{\overline{BC}\sin\alpha}{\sin(\theta-\phi-\triangle AOC)} \quad (25)$$

where

$$\sin(\triangle AOC) = \frac{\overline{BC}\sin\alpha}{\sqrt{\overline{BC}^2+(R-\overline{AB})^2+2\ \overline{BC}\ (R-\overline{AB})\cos\alpha}} \quad (26)$$

The area filled with particles in Stage 3 is given by:

$$S = \frac{1}{2}\ \overline{CE}\ \overline{BC}\sin(\triangle BCE) \quad (27)$$

where

$$\triangle BCE = \pi - (\alpha+(\theta-\phi-\triangle AOD)) \quad (28)$$

Since the cross sectional areas filled with particles at various stages can be determined rigorously, the discharge rate from a flight at any position can be computed by using Equation (5) with the aid of suitable symbolic mathematical software. In this work, the CC - Calculus Calculator software (14) is employed.

EXPERIMENTS AND MODEL VALIDATION

In the experiments using the pilot plant, the following variables were measured: kinetic angle of repose, flight discharge rate, solid axial flowrate, air velocity, average retention time and retention time distribution, and airborne curtain width. The video recorder system and tracers (glass beads and coloured sugar) supplemented by the conventional weighting techniques were employed for the measurements. The detailed experimental procedures have been well documented (12 and 13).

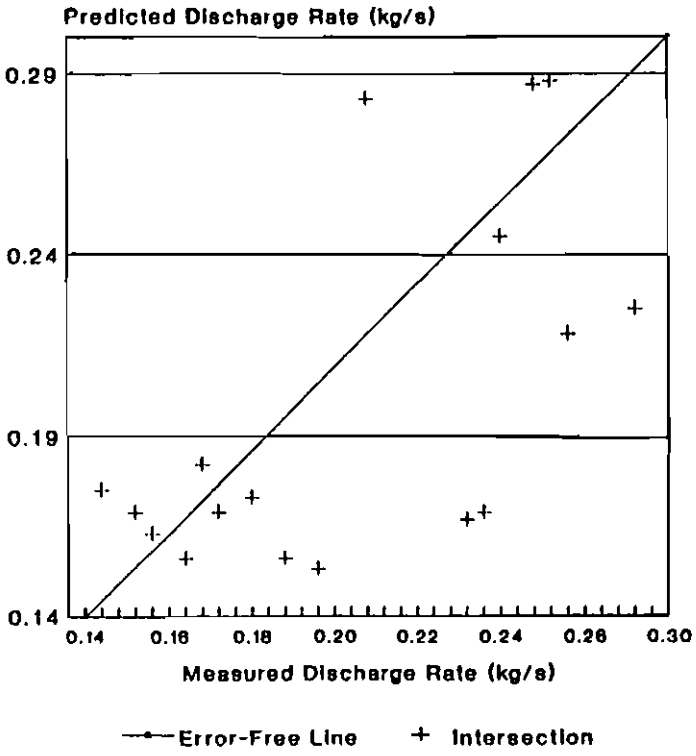

Figure 7: Prediction vs. Measurement (Discharge Rate)

The heart of the model is the flight discharge rate given by Equation (5). It is used for the determination of a variety of important system variables such as solid axial flowrate, airborne solid holdup, voidage and retention time. The computed flight discharge rates are compared with the measured ones in Figure 7. Since the deviations were caused by both the model mismatch as well as the inaccurate measurements (overall measurement error is as high as 33%), the model accuracy could be regarded as acceptable.

The computed retention times are close to, but about 10% longer than the average measured retention times which can be seen from Figure 8. The major factors leading to this error seem to come from bouncing and kilning, which have so far not been rigorously considered in the model. Only a correction factor Γ was introduced to try and handle the bouncing and kilning effects. Obviously, if these two actions are significant, more rigorous methods should be investigated. Further theoretical development and experimental validation work is continuing.

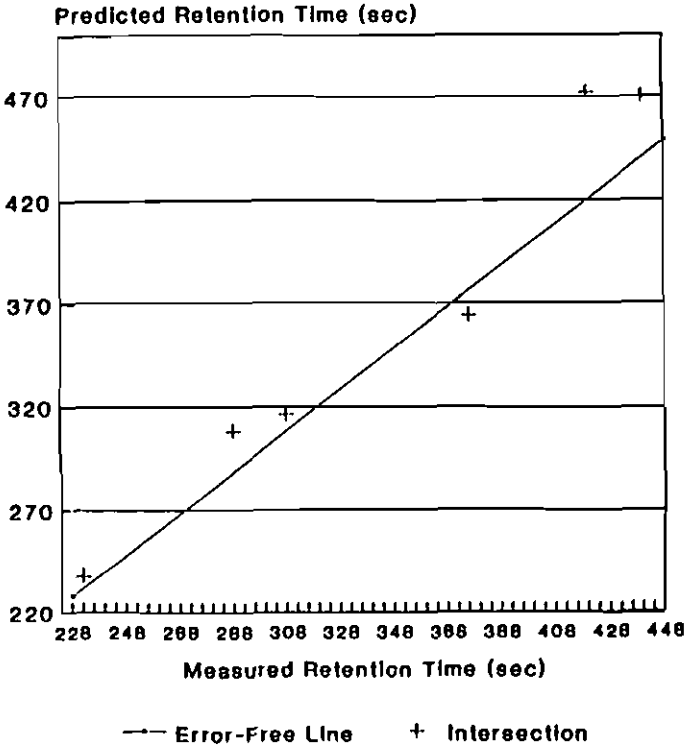

Figure 8: Prediction vs. Measurement (Retention Time)

Table 1: Computed and Measured Curtain Widths

Rotation Rate (rpm)	Flight Position θ (deg)	Falling Height h_t (mm)	Computed Width W_c (mm)	Measured Width W_m (mm)
3	50	107	16.5	15
3	80	107	20.5	22
3	115	107	15.7	13
4.5	50	110	18.8	17
4.5	80	110	23.4	23
4.5	100	110	20.7	25

The computed and measured widths of curtains at various positions and operational conditions are listed in Table 1. A good agreement has been achieved which has confirmed the validity of the application of the extreme value theory. However, it has been observed from the video pictures that the further the position away from a curtain centre, the lower the particle density. That is, the solid density is not uniform within a curtain. This observation has certain implications in rotary drum behaviour.

CONCLUSIONS

The rigorous mathematical model developed in this paper provides an improved prediction of particle transport in rotary dryers in terms of flight discharge rate, retention time, airborne and dense phase solid holdup, particle curtain geometry and voidage, and solid flowrate. The model can be integrated into an overall dynamic model described by a set of partial differential equations developed earlier by the authors (1 and 2). Consequently, a unified theory can be established for investigation of rotary drying dynamics. The model is not only useful in the dynamic study of rotary drying processes, but also provides a sound basis for design of optimal drum configurations by using optimisation techniques. A number of important modelling issues have been verified by using experimental data. The model is in the process of being further validated against more accurate measurements.

Additional studies on bouncing and kilning, particle density distribution within a curtain, shielding effects, and drag forces are needed to address the deficiencies in the current approach.

ACKNOWLEDGMENT

The authors wish to thank Professors J.J. Kelly and D.V. Khakhar for valuable suggestions. The financial assistance of Sugar Research Institute (SRI) of Australia for the establishment of a pilot-scale perspex sugar dryer is gratefully acknowledged. We also wish to express our thanks to Nicholas Earner and Madoc Sheehan for their fruitful experimental results obtained in very tough operational conditions.

NOTATION

a acceleration, m/sec^2
C_D drag coefficient
D_p particle diameter, m
d side length of flight, m
G_a airborne holdup per unit length, kg/m
g gravitational acceleration, m/sec^2
h side length of flight, m; particle falling height, m
h_i particle falling height from the ith flight, m
h_s specified falling distance, m
L dryer length
L_i length in the ith flight delivering particle to next slice, m
M mass holdup per unit length, kg/m
m_p single particle mass, kg
n number of active flights
N total number of flights
R dryer radius, m
R_{eff} effective dryer radius, m
R_D particle discharge rate from flight with unit length, kg/sec m

R_e Reynold number
R_r radius of inner circle (flight-free space), m
S cross sectional area of flight filled with solids, m^2
t_i particle falling time from the ith flight, sec
t_r retention time, sec; min
t_s particle falling time to reach the specified position, sec
V volume filled with particle in flight, m^3
V_p velocity, m/sec
V_s solid flowrate, kg/sec
v_h horizontal velocity, m/sec
v_v vertical velocity, m/sec
W_c computed curtain width, mm
W_m measured curtain width, mm
w_i weighting factor
z spatial variable, m

ℓ side length of solids in flight, m
α flight angle, deg
θ flight position angle, rad
ϕ angle of repose, rad
γ drum slope to horizontal, deg
ϵ voidage
Γ correction factor
ς sliding-rolling ratio
μ coefficient of static friction
ρ_b bulk density, kg/m^3
ρ_s solid density, kg/m^3
ω angle velocity, rad/sec

LITERATURE CITED

1. F.Y. Wang, I.T. Cameron, J.D. Litster and P.L. Douglas, 1993, 'A distributed parameter approach to the dynamics of rotary drying processes', Drying Technology, **11** (7), 1641-1656.

2. F.Y. Wang, I.T. Cameron and J.D. Litster, 1995, 'Further theoretical studies on rotary drying processes represented by distributed systems', Drying Technology, Special Edition on Mathematical Modelling and Numerical Techniques for the Solution of Drying Problems (in press).

3. J.J. Kelly and P. O'Donnell, 1977, 'Residence time model for rotary drums', Trans IChemE, **55**, 243-252.

4. P.G. Glikin, 1978, 'Transport of solids through flighted rotating drums', Trans IChemE, **56**, 120-126.

5. F.A. Kamke and J.B. Wilson, 1986, 'Computer simulation of a rotary dryer, Part I and II', AIChE J, **32** (2), 263-275.

6. A.J. Matchett and M.S. Sheikh, 1990, 'An improved model of particle motion in cascading rotary dryers', Trans IChemE, **68**, Part A, 139-148.

7. S.D. Gupta, D.V. Khakhar and S.K. Bhatia, 1991, 'Axial transport of granular solids in horizontal rotating cylinders, Part I and II', Powder Technology, **67**, 145-151.

8. R.G. Sherritt, R. Caple, L.A. Behie and A.K. Mehrotra, 1993, 'The movement of solids through flighted rotating drums, Part I: Model formulation; Part II: Solid-gas interaction and model validation', Can J Chem Eng, **71**, 337-346; **72**, 240-248.

9. H. Hironsue, 1989, 'Influence of particle falling from flights on volumetric heat transfer coefficient in rotary dryers and coolers', Powder Technology, **59**, 125-128.

10. M.C.J. Hodgson and W.J. Keast, 1984, 'Rotary dryer flight design', Proc Australian Soc Sugar Cane Technologists (ASSCT), 211-218.

11. M.M. Denn, 1980, 'Process Fluid Mechanics', Prentice-Hall, Englewood Cliffs, N.J., 53-56.

12. M. Sheehan, 1993, 'A study on the material transport in a flighted rotary dryer', B.E. Thesis (Honours), The University of Queensland, Brisbane, Australia.

13. N. Earner, 1994, 'The effect of air flow on the movement of solids in rotating drums', B.E. Thesis (Honours), The University of Queensland, Brisbane, Australia.

14. D. Meredith, 1991, 'CC - the Calculus Calculator', Prentice-Hall.